Cardiovascular Diabetology

RESEARCH

Open Access

Epicardial Adipose Tissue and Heterogeneity Parameters Combined with Inflammatory Cells to Predict the Value of Heart Failure with Preserved Ejection Fraction Patients Post Myocardial Infarction

Yu-jiao Song[1†], Xiao-ying Zhao[1†], Lu-jing Wang[1], Ting Ning[1], Ming-tian Chen[1], Pei Liu[1], Si-wen Chen[1] and Xin-xiang Zhao[1*]

Abstract

Background and purpose Epicardial adipose tissue (EAT) comprises three distinct lipid components, each exerting differential effects on cardiovascular diseases. During disease progression, dynamic alterations in lipid composition and spatial distribution contribute to the inherent heterogeneity of EAT. The excessive activation of inflammatory cells may contribute to chronic inflammation, promoting atherosclerosis and cardiac diseases. However, the role of EAT in patients with myocardial infarction (MI) who develop heart failure with preserved ejection fraction (HFpEF) remains unclear. This study aims to quantify the overall and perivascular volumes of EAT using cardiac magnetic resonance (CMR) imaging and assess its heterogeneity, exploring the predictive value of EAT heterogeneity and different EAT volumes combined with inflammatory cells for the occurrence of HFpEF in MI patients with normal left ventricular ejection fraction (LVEF).

Methods This retrospective cohort study enrolled patients diagnosed with MI with preserved LVEF via clinical assessment and CMR at the Second Affiliated Hospital of Kunming Medical University between January 2015 and July 2023. Patients who did not undergo percutaneous coronary intervention (PCI) were followed, with the incidence of HFpEF serving as the primary endpoint. The cohort was stratified into two groups: those without HFpEF and those who developed HFpEF.Cardiac structure, function, EAT volume, and infarct volume parameters were obtained using the CMR post-processing software CVI-42, while EAT heterogeneity parameters entropy were derived using Python software. Independent sample t-tests, non-parametric tests, and chi-square tests were employed to analyze the differences in clinical baseline data and CMR metrics between the two groups. Spearman's rank correlation was

[†]Yu-jiao Song and Xiao-ying Zhao have contributed equally to the work.

*Correspondence:
Xin-xiang Zhao
zhaoxinxiang2918@outlook.com

Full list of author information is available at the end of the article

utilized to analyze the associations between EAT parameters and inflammatory cells, inflammatory markers, and diastolic dysfunction indicators. Furthermore, we conducted univariate and multivariate Cox regression analyses to determine the predictive value of each parameter for the development of HFpEF in MI patients. Time-dependent ROC curves were generated to evaluate the efficacy of each parameter in predicting HFpEF, the AIC values of each parameter and the final model were calculated to evaluate the predictive performance. The optimal cut-off values were identified using time-dependent ROC curves in R software, and Kaplan–Meier event-survival curves were plotted to illustrate the event-free rates based on these optimal thresholds.The median follow-up time was calculated using the reverse Kaplan–Meier method.

Results A total of 203 MI patients with normal LVEF were included, with 74 in the HFpEF group and 129 in the non-HFpEF group. No significant differences were observed between the two groups regarding age, sex, and infarct volume; however, significant statistical differences were noted in BMI, diabetes, renal failure, leukocytes, neutrophils, monocytes, total EAT, EAT entropy, left ventricular EAT (LV EAT), left atrial end-systolic volume (LAESV), triglycerides, NHR, MHR and LACI(Left atrioventricular coupling index) ($P < 0.05$). Both overall and local EAT volumes showed a positive correlation with leukocytes and monocytes,as well as with the inflammatory markers MHR and SIRI. Furthermore, EAT volume exhibited a positive correlation with the LACI, a marker of diastolic dysfunction. Univariate and multivariate Cox regression analyses indicated that BMI, diabetes, monocyte, LV EAT, and EAT entropy are independent risk factors for HFpEF. And the AIC value of the multivariate regression model was the smallest.Further time-dependent ROC analysis revealed that the maximum AUC for BMI was 0.67, while the AUC for LV EAT was 0.63, and EAT entropy was 0.60, the maximum AUC for monocyte was 0.70, and the combined prediction of LV EAT and EAT entropy had a maximum AUC of 0.70. After a median follow-up of 34 months, Kaplan–Meier survival curves demonstrated that LV EAT greater than 21.23 mL was associated with the occurrence of HFpEF, whereas EAT entropy was not.

Conclusions In patients with chronic MI, normal LVEF, and no prior PCI, the occurrence of HFpEF is not correlated with infarct volume; however, BMI, diabetes, monocyte, LV EAT, and EAT entropy are independent risk factors for HFpEF with significant predictive value, with the highest predictive efficacy observed monocyte and when combining EAT entropy and LV EAT. Additionally, both overall and local EAT volumes exhibit a moderate positive correlation with leukocytes,monocytes and inflammatory markers, and were also positively correlated with diastolic dysfunction. This suggests that, in clinical practice, beyond traditional indicators, there should be an increased focus on EAT heterogeneity and perivascular EAT in MI patients with normal LVEF who have not undergone PCI to to reduce the incidence of HFpEF.

Keywords Epicardial adipose tissue, HFpEF, Myocardial infarction, Cardiac magnetic resonance, Entropy

Introduction

MI results from the rupture or erosion of fragile, lipid-laden chronic atherosclerotic coronary plaques, leading to acute interruption of myocardial blood flow and ischemic myocardial necrosis, which is associated with high morbidity and mortality worldwide [1]. The pathological remodeling of the heart following MI promotes the onset of HF, the incidence of which has been increasing annually [2]. Despite significant reductions in mortality risk due to advancements in reperfusion therapy and secondary prevention strategies, patients who experience MI remain at risk for developing HF, and the occurrence and progression of HF post-MI continue to be major factors contributing to poor prognosis [3]. Historically, the most common type of HF has been HFrEF; however, with advancements in pharmacotherapy, the incidence and prognosis of HFrEF have markedly improved [4]. In contrast, HFpEF has emerged as a leading cause of increased morbidity and mortality in industrialized nations, accounting for over 50% of all HF hospitalizations. Due to its considerable clinical heterogeneity, any factor that can lead to myocardial fibrosis or impair diastolic function may contribute to the development of HFpEF [5]. Consequently, treatment strategies for HFpEF are complex and have garnered significant clinical attention in recent years, yet there remains a lack of clinical predictive models for HFpEF following MI [6].

Obesity has been established as a significant risk factor for the development of HF [7], with increased visceral fat levels further exacerbating myocardial dysfunction and fibrosis, thereby promoting the onset and progression of HFpEF. Recent studies have increasingly focused on visceral fat, particularly EAT, which, as a metabolically active fat depot in direct contact with the myocardium and coronary arteries, can engage in local interactions and direct cellular crosstalk. Under healthy conditions, EAT exhibits protective functions; however, in pathological states, it can become a critical factor in promoting inflammation and fibrosis [8]. EAT contributes to cardiac remodeling by secreting inflammatory

cytokines, releasing excess fatty acids, and increasing the mechanical load on the myocardium [9]. Inflammation plays a crucial role in atherosclerosis, and EAT, as a pro-inflammatory tissue, influences the formation of coronary plaques [10]. Numerous studies have demonstrated that due to the unique location and endocrine activity of EAT, it has a direct impact on inflammation and fibrosis in both the myocardium and coronary arteries [4]. The correlation between EAT and coronary artery disease is well-established, and the functional efficacy of EAT may vary by anatomical location; however, the role of EAT in the prognosis of MI patients remains unclear. Prior foundational research has established that EAT comprises three distinct lipid components, each exerting differential effects on cardiovascular disease. Furthermore, the composition and distribution of these components undergo dynamic alterations throughout the disease course, thereby contributing to the heterogeneity of EAT. Entropy, a parameter quantifying tissue homogeneity and distributional uncertainty, has been previously employed and validated in the context of cardiovascular disease.CMR as a novel assessment tool, is increasingly utilized in the diagnosis of cardiovascular diseases and is regarded as the "gold standard" for measuring EAT [11]. It not only quantifies the heterogeneity of EAT but also provides comprehensive information regarding all tissue characteristics post MI. Consequently, this research holds significant value in studying the occurrence of HFpEF following MI. However, there is currently a lack of studies focusing on EAT in MI patients. The objective of this study is to utilize CMR to measure the overall and perivascular volumes of EAT, assess its heterogeneity, and explore the correlation between EAT and inflammatory cells, as well as the predictive value of both in the development of HFpEF in MI patients.

Methods

Study populations

This study is a historical cohort investigation. We collected data from patients diagnosed with MI at the Second Affiliated Hospital of Kunming Medical University between January 2015 and August 2023. The examination was conducted at least three months after the onset of acute MI, with CMR imaging revealing distinct MI lesions. Additionally, echocardiographic assessments and relevant laboratory tests were performed. Following CMR examination, patients underwent outpatient follow-up every three months, encompassing symptom assessment, physical examination, and BNP testing. Transthoracic echocardiography was repeated every six months until the study's conclusion. For patients who died before the study's end, the cause of death was evaluated by reviewing medical records, relevant examinations, and death certificates. The assessment strictly adhered to the ESC heart failure guidelines, with a focus on heart failure hospitalization. Two researchers independently analyzed echocardiographic parameters to minimize bias. A panel of three researchers reviewed all potential endpoint events to ensure they met predefined criteria. All research personnel received standardized training. Data were entered into an electronic system in real-time and were regularly audited. The primary endpoint was the occurrence of HFpEF.The study protocol was approved by the hospital's ethics committee (Approval No.审-PJ-科-2023-30).

The diagnosis of HFpEF is established according to the Heart Failure Association (HFA)-PEFF diagnostic algorithm [12], specifically as follows: 1. The patient presents with clinical symptoms and signs: Typical symptoms include dyspnea (worsened by activity, orthopnea), fatigue, and reduced exercise tolerance. Signs include pulmonary crackles, lower extremity edema, jugular venous distension, and a positive hepatojugular reflux. 2. Echocardiographic parameters and other imaging examinations: LVEF: ≥ 50%; Diastolic dysfunction is present (meeting at least two of the following): Elevated E/e′ ratio: septal or lateral E/e′ ≥ 13 (tissue Doppler); Left atrial enlargement: left atrial volume index > 34 mL/m^2; Left ventricular hypertrophy: interventricular septum or left ventricular posterior wall thickness ≥ 12 mm; Tricuspid regurgitation peak velocity: > 2.8 m/s [13]. Chest X-ray reveals pulmonary edema. 3. Natriuretic peptide levels: Elevated BNP or NT-proBNP: BNP > 35 pg/mL or NT-proBNP > 125 pg/mL.

The criteria for diagnosing chronic MI are delineated as follows [14]: (1) the presence of abnormal Q waves on the electrocardiogram, whether symptomatic or asymptomatic, in the absence of non-ischemic causes; (2) imaging evidence demonstrating the loss of viable myocardium, consistent with an ischemic origin; (3) pathological findings that confirm the presence of MI. A diagnosis can be established if any one of these criteria is satisfied.

Exclusion criteria included: (1) the presence of heart failure at baseline; (2) the onset of HFrEF during follow-up (based on NYHA classification, BNP or NT-proBNP levels, echocardiographic structural and/or functional alterations, or reduced ejection fraction); (3) the existence of severe valvular heart disease, congenital heart disease, cardiomyopathy, or other cardiovascular conditions at baseline or during follow-up; (4) insufficient image quality for post-processing analysis; (5) loss to follow-up (Fig. 1).

Inspection method

Utilizing the Philips Achieva 3.0 T MRI system, I conducted head-up scans on patients employing MRI-compatible precordial lead electrocardiogram gating technology alongside a 16-channel phased-array

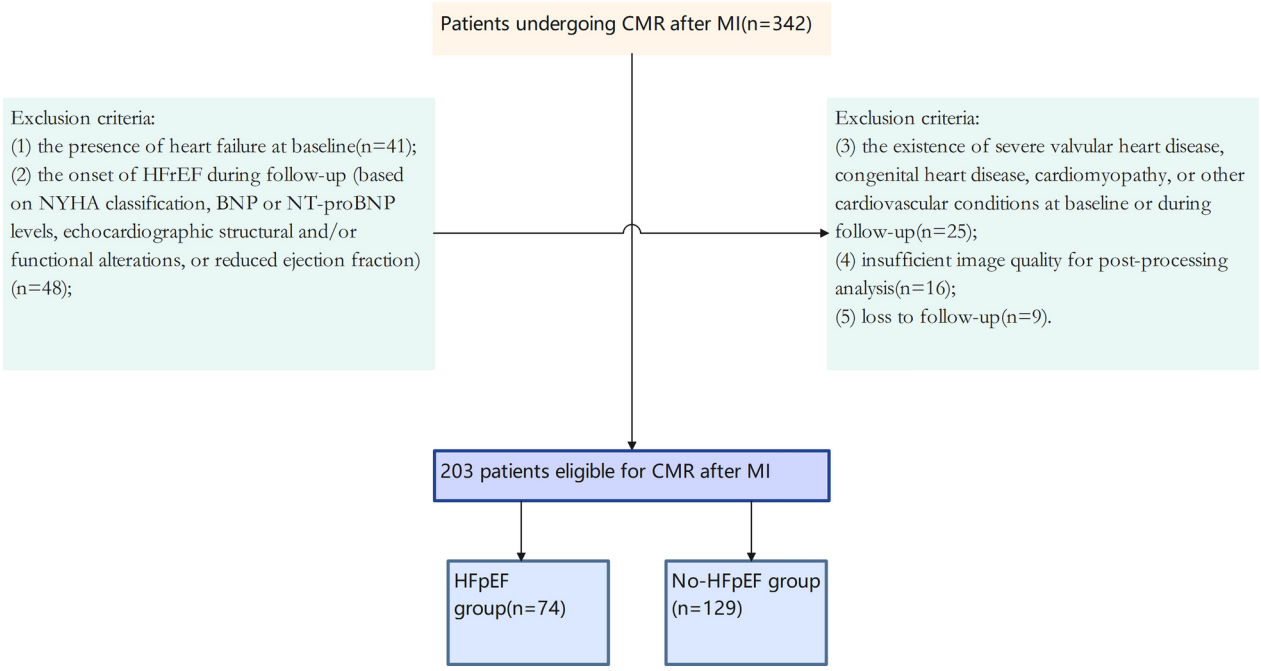

Fig. 1 Study flowchart. *CMR* cardiac magnetic resonance imaging, *MI* myocardial infarction, *HFpEF* heart failure with preserved ejection fraction

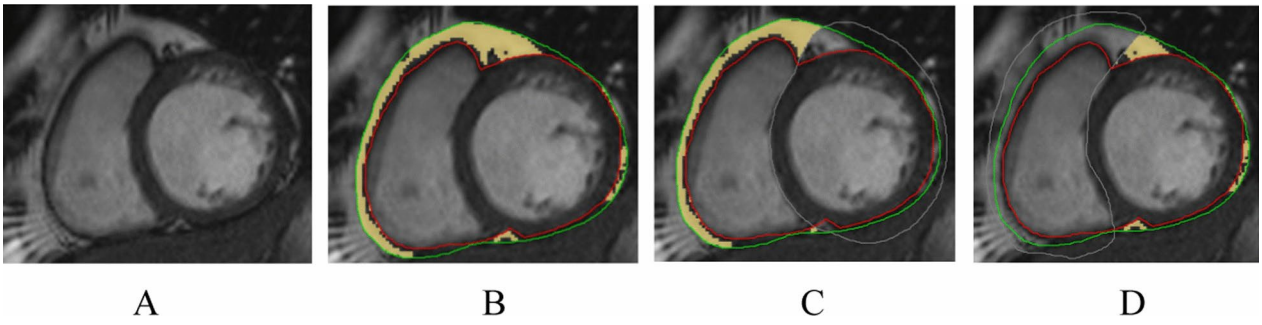

Fig. 2 **A**–**D** Schematic diagram for the measurement of total and local EAT volume. *EAT* epicardial adipose tissue

cardiac coil to acquire CMR images. I implemented a rapid steady-state free precession sequence to capture both short-axis and long-axis cardiac cine images, which included the four-chamber long-axis view, the left ventricle two-chamber long-axis view, and the two-chamber short-axis view. The acquisition parameters were as follows: TE 1.61 ms, TR 3.22 ms; flip angle 45°, field of view (FOV): 350 mm × 350 mm, with a single acquisition capturing 25 cardiac cycles per slice and a slice thickness of 8 mm. For delayed enhancement imaging, I administered gadobutrol (0.2 mmol/kg, flow rate 3 mL/s) via a high-pressure injector through the antecubital vein, followed by delayed scans performed 3–15 min later to obtain multi-axis late gadolinium enhancement (LGE) images, with primary acquisition parameters of TE 2.41 ms, TR 5.11 ms, flip angle 25°, FOV: 320 mm × 320 mm, and slice thickness of 10 mm.

Post-processing analysis of CMR images

Using the third-party post-processing software CVI 42 (Circle Cardiovascular Imaging, Canada), I utilized the tissue signal intensity module within the steady-state free precession (SSFP) sequence, which is commonly employed in routine cardiac imaging "cine" sequences. Manually delineated the boundaries of the EAT images on the short-axis slices at the end of diastole, marking the epicardial layer in red and the fat wall layer in green. High-signal adipose tissue was highlighted in yellow using a signal intensity threshold, while ensuring the exclusion of the coronary arteries and pericardial fat (Fig. 2A–D). The interventricular septum served as a demarcation for collecting the pericardial EAT from both ventricles. EAT image analysis was performed by YJ.S and XY.Z in consultation. LACI was defined as the ratio of LA end-diastolic volume to LV end-diastolic volume, as assessed by CMR. LV volumes were measured from

short-axis cine images, while LA volumes were measured from two- and four-chamber views.

Entropy analysis was conducted utilizing a program developed in Python (MathWorks, version 3.8, Natick, MA). Initially, I delineated the EAT region on short-axis cine images in DICOM format using CVI 42. The myocardial signal intensity for each voxel was automatically extracted, and entropy was computed using the formula previously established by Shannon [15] (Fig. 3A, B). The entropy values were constrained within a range of 0 to 10, where 0 signifies a completely homogeneous distribution of EAT, while 10 indicates the most heterogeneous distribution of EAT [16].

$$Entropy = -\sum_{i=1}^{n} P\left(x_i\right) \log_b P\left(x_i\right),$$

P(xi) represents the probability distribution of signal intensity, with xi denoting the signal intensity and b being an arbitrarily selected base. Signal intensity was normalized according to a predetermined range (from 0 to 1024 for each patient) and scaled from 0 to 10. Furthermore, histogram features characterizing the signal intensity distribution across the region of interest were extracted. To evaluate reproducibility, this quantitative analysis was performed by three independent observers to ensure consistency (YJ.S., XY.Z., and XX.Z.—radiologists with over three years of experience in cardiac MRI).

Statistical methods

Statistical analyses were performed using SPSS version 22.0 (IBM Corporation, Armonk, NY, USA), Prism GraphPad version9.3.1 (GraphPad Software, La Jolla, CA, USA), MedCalc version 20.1.0 (MedCalc Software Ltd, Ostend, Belgium) and R language. Categorical variables were evaluated using the χ^2 test. For the assessment of continuous variables across three groups, normally distributed data were analyzed with independent samples t-test, presented as $x \pm s$. Non-normally distributed continuous data were examined using the rank-sum test, expressed as the median and interquartile range M (P25, P75). Variables demonstrating a P value < 0.05 between the two patient cohorts and deemed relevant to HFpEF were incorporated into a univariate Cox regression analysis. Indicators with a P value < 0.05 in the univariate analysis underwent collinearity assessment. All variables exhibited variance inflation factors < 5, indicating an absence of multicollinearity. These variables were subsequently employed in a multivariate Cox stepwise regression to ascertain the risk factors associated with HFpEF development. The AIC values of each parameter and the final model were calculated to evaluate the prediction performance. Time-dependent receiver operating characteristic (ROC) curves were generated, and the area under the curve (AUC) was computed at various time points to identify prognostic parameters and establish the optimal threshold for predicting the primary endpoint events. The optimal cut-off values were identified using time-dependent ROC curves in R software, and Kaplan–Meier event-survival curves were plotted to illustrate the event-free rates based on these optimal thresholds.The median follow-up time was calculated using the reverse Kaplan–Meier method.Additionally, employ Spearman correlation analysis to assess the relationship between total EAT, LV EAT, RV EAT, and various inflammatory markers and

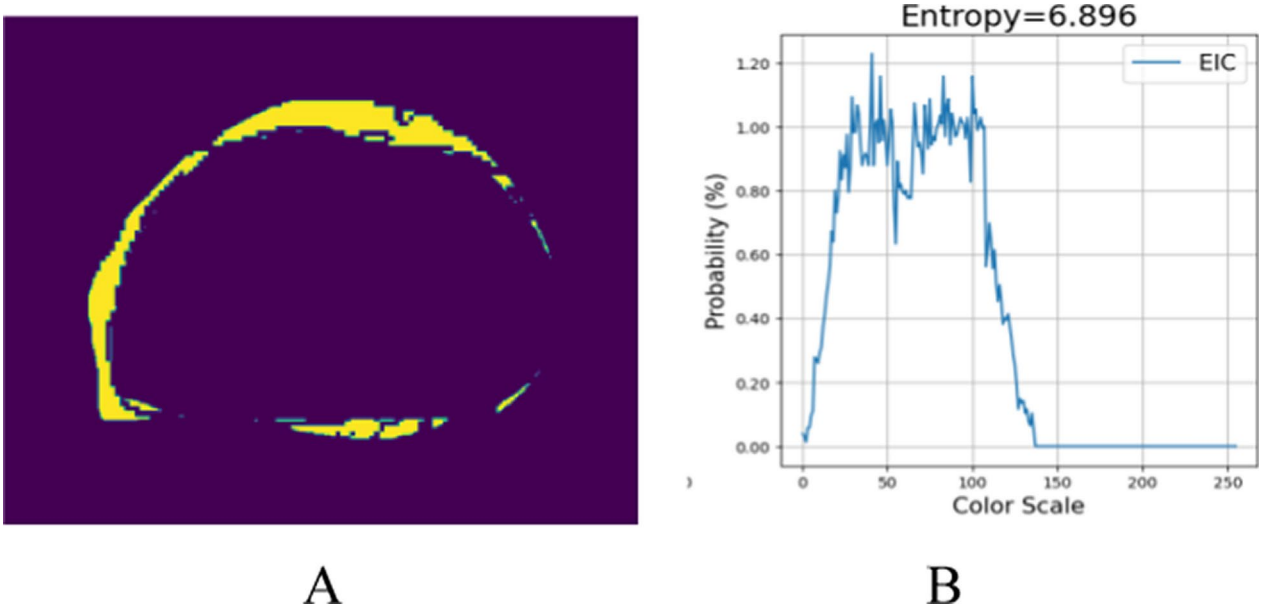

Fig. 3 **A**, **B** Schematic diagram for the measurement of EAT entropy. *EAT* epicardial adipose tissue

diastolic dysfunction index. A P value of < 0.05 is considered statistically significant.

Results

Comparison of general data between the two groups

A total of 203 eligible MI patients were ultimately included in the study, of which 74 developed HFpEF, while 129 did not.

In the HFpEF group, the BMI was 24.40 (22.23, 26.73) compared to 23.40 (21.60, 25.55) (kg/m^2). The prevalence of diabetes was 29 (39.19%) versus 27 (20.93%). Renal failure was observed in 7 (9.46%) versus 3 (2.33%). The white blood cell count was 7.38 (6.15, 9.02) versus 7.12 (5.96, 7.95) (10^9/L), while neutrophils were 4.58 (3.59, 5.77) versus 4.06 (3.22, 4.81) (10^9/L). Monocytes were recorded at 0.51 (0.38, 0.65) versus 0.45 (0.37, 0.53) (10^9/L),NHR were 0.24(0.17,0.34) versus 0.21(0.16, 0.27), MHR were 0.03(0.02,0.04) versus 0.02(0.02,0.03).The total EAT volume was 69.43 ± 21.21 versus 62.18 ± 19.93 (mL), with LV EAT at 24.81 ± 7.39 versus 18.45 (13.03, 25.30) (mL) and RV EAT at 44.61 ± 15.03 versus 40.81 ± 13.68 (mL). The LAESV was 56.18 (42.13, 73.00) versus 51.24 (39.46, 64.44) (mL), LACI were 23.45(15.49, 33.42) versus 19.23(15.19, 26.29)(%)both significantly higher than in the non-HFpEF group. However, EAT entropy was 6.40 (6.22, 6.86) versus 6.75 (6.26, 7.15), and triglycerides (TG) were 1.40 (0.86, 2.05) versus 1.63 (1.20, 2.40), both lower in the non-HFpEF group ($P < 0.05$). No significant statistical differences were observed between the two groups regarding sex, age, smoking history, hypertension history, systolic blood pressure, diastolic blood pressure, pulse pressure, NYHA classification, LDL, HDL, TC, lymphocytes, eosinophils, basophils, red blood cells, LHR, NLR, SIRI, urea, creatinine, RV EAT, EAT/BSA, LVEF, LADSV, end-diastolic volume index, end-systolic volume index, cardiac output, cardiac index, infarct area, LV global strain, mitral regurgitation, tricuspid regurgitation, aortic regurgitation, pulmonary hypertension, the number of diseased vessels and medication situation ($P > 0.05$) (Table 1 and Fig. 4).

Analysis of the correlation between EAT and inflammatory cells, inflammatory markers, and diastolic dysfunction indicators.

Total EAT, LV EAT, and RV EAT exhibited mild-to-moderate positive correlations with white blood cell count, monocyte count, MHR, SIRI, and LACI. RV EAT also showed a moderate positive correlation with LHR ($r = 0.563$, $p = 0.041$). Notably, total EAT demonstrated the strongest correlations with monocyte count ($r = 0.658$, $P < 0.001$), MHR ($r = 0.511$, $P < 0.001$), and SIRI ($r = 0.323$, $p = 0.041$), while RV EAT exhibited the most robust correlations with white blood cell count ($r = 0.469$, $P < 0.001$) and LACI ($r = 0.313$, $P < 0.001$) (Table 2 and Fig. 5).

Analysis of independent risk factors for HFpEF in MI patients

The indicators that showed significant differences between the two groups and were considered predictive of HFpEF occurrence were utilized as independent variables, with HFpEF serving as the dependent variable. Univariate Cox regression analysis revealed that the risk factors for HFpEF included renal failure, diabetes, BMI, monocytes, MHR, total EAT, LV EAT, and EAT entropy ($P < 0.05$).

In the multivariable Cox regression model, LV EAT (HR 1.102, 95% CI 1.026–1.183), EAT entropy (HR 0.338, 95% CI 0.181–0.630), diabetes (HR 2.248, 95% CI 1.351–3.741), BMI (HR 1.086, 95% CI 1.018–1.159), and monocyte count (HR: 1.839, 95% CI 1.181–2.863) were identified as independent predictors of HFpEF incidence, among them, the AIC value of the model of multivariate analysis was the smallest, suggesting that the model had better prediction performance (Table 3). Time-dependent ROC analysis revealed a maximum AUC of 0.67 for BMI, 0.63 for LV EAT, and 0.60 for EAT entropy. The combined prediction model of LV EAT and EAT entropy yielded a maximum AUC of 0.70 (Fig. 6). Kaplan–Meier survival analysis, with a median follow-up of 34 months (range, 2–120 months), demonstrated that LV EAT volume greater than 21.23 mL was associated with HFpEF, whereas EAT entropy was not (Fig. 7).

Discussion

To our knowledge, this is the first investigation into the correlation between overall and regional EAT, EAT entropy, and various inflammatory markers in patients with chronic MI who did not undergo PCI, as well as their predictive value for HFpEF. The main findings of this study are as follows: (1) BMI, diabetes, renal failure, leukocytes, neutrophils, monocytes, total EAT, LV EAT, RV EAT, and LAESV were all significantly higher in the HFpEF group compared to the non-HFpEF group, while EAT entropy and TG were lower in the HFpEF group; (2) Both global and regional EAT demonstrated mild to moderate positive correlations with leukocyte and monocyte counts, as well as inflammatory markers. Furthermore, EAT volume exhibited a mild positive correlation with LACI, a marker of diastolic dysfunction; (3) LV EAT, EAT entropy, BMI, and diabetes were identified as independent risk factors for HFpEF, with EAT entropy and LV EAT demonstrating the greatest combined predictive efficacy.

Diabetes, BMI with HFpEF post-MI

Obesity is associated with various cardiovascular diseases, including coronary artery disease, atrial fibrillation, and HF, making it one of the most significant risk factors for cardiovascular conditions. Patients with

Table 1 Comparison of clinical baseline data between two groups

Parameters	Total (n = 203)	No-HFpEF (n = 129)	HFpEF (n = 74)	χ^2/t/Z value	*P* value
Male [n(%)]	148 (73.40)	97 (75.19)	51 (68.92)	0.937	0.333
Age (years)	55.13 ± 13.17	53.81 ± 13.622	57.45 ± 12.09	1.908	0.058
BMI (kg/m^2)	23.70 (21.90, 26.20)	23.40 (21.60, 25.55)	24.40(22.23, 26.73)	− 1.986	0.047*
Smoke [n (%)]	92 (45.32)	56 (43.41)	36 (48.65)	0.521	0.471
Hypertension [n (%)]	114 (56.16)	70 (54.26)	44 (59.46)	0.158	0.166
Diabetes [n (%)]	56 (27.59)	27 (20.93)	29 (39.19)	7.848	0.005*
Systolic pressure (mmHg)	130.00 ± 21.47	130.32 ± 21.68	129.46 ± 21.24	− 0.273	0.785
Diastolic pressure (mmHg)	80.66 ± 14.53	80.77 ± 13.98	80.47 ± 15.54	− 0.139	0.890
Pulse pressure (mmHg)	47.00 (39.00, 58.00)	46.00 (38.50, 56.50)	47.00 (39.75, 59.00)	− 0.283	0.777
NYHA				5.952	0.051
I	120 (59.11)	77 (59.69)	43 (58.11)		
II	77 (37.93)	51 (39.53)	26 (5.13)		
III	6 (2.96)	1 (0.78)	5 (6.76)		
Renal failure [n (%)]	10 (4.93)	3 (2.33)	7 (9.46)	5.110	0.024*
LDL (mmol/L)	2.37 (1.86, 3.18)	2.37 (1.87, 3.17)	2.29 (1.86, 3.20)	− 0.567	0.571
HDL (mmol/L)	1.11 (0.94, 1.24)	1.10 (0.95, 1.26)	1.13 (0.92, 1.20)	− 0.562	0.574
TC (mmol/L)	4.04 (3.33, 4.88)	4.03 (3.35, 4.88)	4.10 (3.23, 4.92)	0.528	0.598
TG (mmol/L)	1.56 (1.12, 2.24)	1.63 (1.20, 2.40)	1.40 (0.86, 2.05)	− 2.105	0.035*
NHR	0.22 (0.16, 0.28)	0.21 (0.16, 0.27)	0.24 (0.17, 0.34)	− 2.582	0.010*
MHR	0.02 (0.02, 0.03)	0.02 (0.02, 0.03)	0.03 (0.02, 0.04)	− 2.223	0.026*
LHR	0.09 (0.07, 0.12)	0.09 (0.06, 0.12)	0.10 (0.07, 0.14)	− 1.752	0.080
NLR	2.31 (1.78, 3.23)	2.22 (1.78, 3.07)	2.50 (1.75, 3.50)	− 1.059	0.290
SIRI	1.05 (0.75, 1.64)	1.02 (0.73, 1.46)	1.20 (0.81, 1.96)	− 1.804	0.071
White blood cell (10*9/L)	7.18 (6.01, 8.33)	7.12 (5.96, 7.95)	7.38 (6.15, 9.02)	− 2.256	0.024*
Neutrophils (10*9/L)	4.20 (3.34, 5.26)	4.06 (3.22, 4.81)	4.58 (3.59, 5.77)	− 2.494	0.013*
Lymphocyte (10*9/L)	1.82 (1.37, 2.25)	1.80 (1.34, 2.19)	1.84 (1.40, 2.35)	− 1.251	0.211
Monocyte (10*9/L)	0.46 (0.37, 0.57)	0.45 (0.37, 0.53)	0.51 (0.38, 0.65)	− 2.176	0.030*
Eosinophils (10*9/L)	0.12 (0.07, 0.20)	0.12 (0.07, 0.22)	0.11 (0.58, 0.17)	− 1.835	0.067
Basophil granulocyte (10*9/L)	0.02 (0.02, 0.04)	0.02 (0.02, 0.04)	0.02 (0.01, 0.03)	− 1.109	0.268
Red blood cell (10*9/L)	4.84 (4.46, 5.24)	4.82 (4.45, 5.24)	4.86 (4.50, 5.24)	− 0.236	0.814
Urea (mmol/L)	4.93 (4.16, 6.10)	4.88 (4.05, 5.87)	5.24 (4.37, 6.36)	− 1.255	0.210
Creatinine (μmol/L)	78.00 (68.00, 92.00)	77.00 (68.00, 90.50)	80.00 (66.50, 93.00)	− 0.651	0.515
Total EAT (mL)	64.82 ± 20.65	62.18 ± 19.93	69.43 ± 21.21	2.437	0.016*
EAT/BSA	37.68 (26.95, 46.72)	37.50 (26.21, 45.94)	39.48 (29.78, 50.48)	− 1.631	0.103
LV EAT (mL)	22.62 ± 8.02	21.37 ± 8.13	24.81 ± 7.39	3.003	0.003*
RV EAT (mL)	42.20 ± 14.27	40.81 ± 13.68	44.61 ± 15.03	1.838	0.068
EAT entropy	6.53 (6.25, 7.03)	6.75 (6.26, 7.15)	6.40 (6.22, 6.86)	− 2.242	0.025*
LVEF (%)	60.00 (52.00, 65.00)	62.00 (47.50, 67.00)	57.50 (55.00, 63.00)	− 1.173	0.241
LADSV (mL)	27.11 (18.42, 37.56)	26.24 (17.97, 36.75)	29.14 (21.18, 40.83)	− 1.654	0.100
LAESV(mL)	53.18 (40.42, 67.38)	51.24 (39.46, 64.44)	56.18 (42.13, 73.00)	− 2.033	0.042*
EDVI(mL/m2)	75.09 (61.53, 93.83)	75.88 (61.18, 94.33)	74.72 (61.32, 93.31)	− 0.159	0.874
ESVI(mL/m2)	36.09 (25.76, 55.56)	35.35 (23.69, 57.58)	38.23 (29.90, 52.71)	− 0.997	0.319
LACI(%)	19.65 (15.24, 28.28)	19.23(15.19,26.29)	23.45 (15.49, 33.42)	− 2.316	0.021*
CO(L/min)	4.29 ± 1.52	4.25 ± 1.46	4.35 ± 1.62	0.436	0.663
CI (L/(min m^2))	2.50 (1.98, 3.07)	2.48 (1.99, 3.05)	2.57 (1.91, 3.08)	− 0.309	0.757
IS(%)	13.72 (7.02, 20.50)	13.45 (5.73, 20.88)	13.78 (9.20, 20.15)	− 0.443	0.658
GRS(%)	23.33 (16.97, 30.38)	24.60 (16.55, 30.14)	22.23 (17.92, 31.17)	− 0.592	0.554
GCS(%)	− 16.0 6(− 18.74, − 12.08)	− 16.38 (− 19.24, − 10.98)	− 15.84 (− 17.92, − 13.55)	− 0.216	0.829
GLS(%)	− 11.15 ± 3.69	− 11.04 ± 3.94	− 11.34 ± 3.23	− 0.571	0.568
Mitral regurgitation [n (%)]				3.587	0.310
No	75 (36.95)	53 (41.09)	22 (29.73)		
Little	21 (10.34)	12 (9.30)	9 (12.16)		
Mild	100 (49.26)	61 (47.29)	39 (52.70)		

Table 1 (continued)

Parameters	Total (n = 203)	No-HFpEF (n = 129)	HFpEF (n = 74)	χ^2/t/Z value	*P* value
Moderate	7 (3.45)	3 (2.33)	4 (5.41)		
Tricuspid regurgitation [n (%)]				3.247	0.355
No	79 (38.92)	53 (41.09)	26 (35.14)		
Little	14 (6.90)	8 (6.20)	6 (8.11)		
Mild	106 (52.22)	67 (51.94)	39 (52.70)		
Moderate	4 (1.97)	1 (0.78)	3 (4.05)		
Aortic regurgitation [n (%)]				0.850	0.838
No	125 (61.58)	81 (62.79)	44 (59.46)		
Little	38 (18.72)	22 (17.05)	16 (21.62)		
Mild	38 (18.72)	25 (19.38)	13 (17.57)		
Moderate	2 (0.99)	1 (0.78)	1 (1.35)		
Pulmonary hypertension [n (%)]	18 (8.87)	9 (6.98)	9(12.16)	1.565	0.211
Pathological vascular branch [n (%)]				7.445	0.059
0	24 (11.82)	19 (14.73)	5 (6.76)		
1	112 (55.17)	75 (58.14)	37 (50.00)		
2	51 (25.12)	28 (21.71)	23 (31.08)		
3	16 (7.88)	7 (5.43)	9 (12.16)		
Pathological vascular [n (%)]					
LAD	123 (60.59)	74 (57.36)	49 (66.22)	1.543	0.214
LCX	69 (33.99)	39 (30.23)	30 (40.54)	2.227	0.136
RCA	70 (34.49)	39 (30.23)	31 (41.89)	2.830	0.093
β-blockers [n (%)]	179 (88.18)	112 (86.82)	67 (90.54)	0.624	0.430
ARNI [n (%)]	59 (29.06)	35 (27.13)	24 (32.43)	0.641	0.423
ACEI [n (%)]	65 (32.02)	37 (28.68)	28 (37.84)	1.811	0.178
ARB [n (%)]	27 (13.31)	18 (13.95)	9 (12.16)	0.131	0.718
Statins [n (%)]	189 (93.10)	118 (91.47)	71 (95.95)	1.465	0.226
Diuretics [n (%)]	63 (31.03)	38 (29.46)	25 (33.78)	0.411	0.521
ASA [n (%)]	173 (85.22)	111 (86.05)	62 (83.78)	0.191	0.662
CLO [n (%)]	129 (63.55)	82 (63.57)	47 (63.51)	0.000	0.994
TMZ [n (%)]	82 (40.39)	51 (39.53)	31 (41.89)	0.109	0.742
DIG [n (%)]	16 (7.88)	10 (7.75)	6 (8.12)	0.008	0.928

BMI body mass index, *NYHA* New York Heart Association, *LDL* low-density lipoprotein, *HDL* high-density lipoprotein cholesterol, *TC* total cholesterol, *TG* triglyceride, *NHR* Neutrophil/high-density lipoprotein cholesterol ratio, *MHR* mononuclear cell/high-density lipoprotein cholesterol ratio, *LHR* lymphocyte/high-density lipoprotein cholesterol ratio, *NLR* neutrophils/lymphocytes ratio, *SIRI* systemic immune-inflammation index, *EAT* epicardial adipose tissue, *LV* left ventricular, *RV* right ventricular, *BSA* body surface area, *LVEF* left ventricular ejection fraction, *LADSV* left atrial diastolic-systolic volume, *LAESV* left atrial end-systolic volume, *EDVI* end diastolic volume index, *ESVI* end systolic volume index, *LACI* left atrial-ventricular coupling index, *CO* cardiac output, *CI* cardiac index, IS infarct size, *GRS* global radial strain, *GCS* global circumferential strain, *GLS* global longitudinal strain, *LAD* left anterior descending artery, *LCX* left circumflex, *RCA* right coronary artery, *ARNI* angiotensin receptor-neprilysin inhibitor, *ACEI* angiotensin converting enzyme inhibitor, *ARB* angiotensin II receptor blockers, *ASA* aspirin, CLO Cloxicillin, *TMZ* temozolomide, *DIG* digoxin

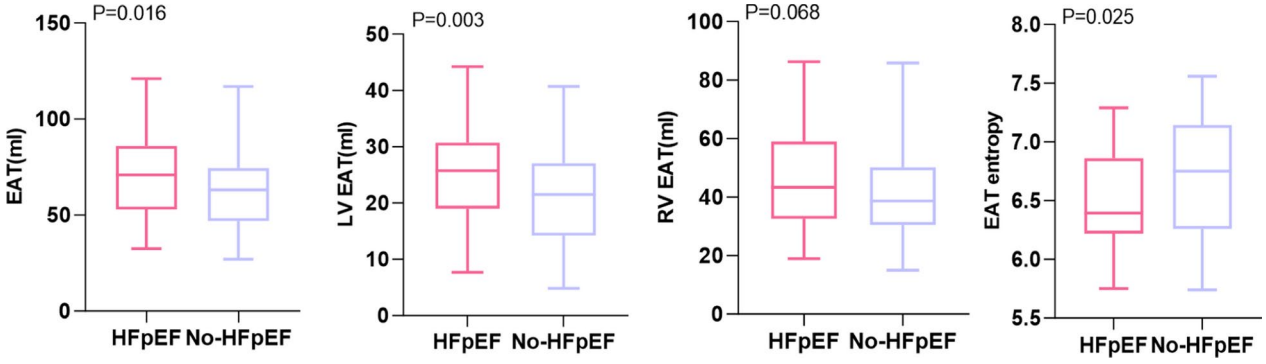

Fig. 4 Comparison of EAT indicators between the two groups. *EAT* epicardial adipose tissue, *HFpEF* heart failure with preserved ejection fraction, *LV* left ventricular, *RV* right ventricular

Table 2 Correlation between EAT and Inflammation indicators and LACI

Parameters	EAT		LV EAT		RV EAT	
	RS	*P* value	RS	*P* value	RS	*P* value
White blood cell (10*9/L)	0.457	< 0.001*	0.359	< 0.001*	0.469	< 0.001*
Neutrophils (10*9/L)	− 0.083	0.242	− 0.039	0.577	− 0.090	0.200
Lymphocyte (10*9/L)	0.091	0.197	0.078	0.267	0.084	0.233
Monocyte (10*9/L)	0.658	< 0.001*	0.583	< 0.001*	0.632	< 0.001*
Eosinophils (10*9/L)	− 0.009	0.895	− 0.022	0.760	0.007	0.921
Basophil granulocyte (10*9/L)	− 0.032	0.650	− 0.028	0.693	− 0.031	0.657
Red blood cell (10*9/L)	− 0.002	0.974	0.013	0.850	0.013	0.843
NHR	− 0.115	0.103	− 0.066	0.348	− 0.122	0.084
MHR	0.511	< 0.001*	0.456	< 0.001*	0.489	< 0.001*
LHR	0.054	0.441	0.066	0.348	0.563	0.041*
NLR	− 0.113	0.109	− 0.066	0.348	− 0.118	0.094
SIRI	0.323	< 0.001*	0.318	< 0.001*	0.298	< 0.001*
LACI (%)	0.312	< 0.001*	0.250	< 0.001*	0.313	< 0.001*

EAT epicardial adipose tissue, *LV* left ventricular, *RV* right ventricular, *NHR* neutrophil/high-density lipoprotein cholesterol ratio, *MHR* mononuclear cell/high-density lipoprotein cholesterol ratio, *LHR* lymphocyte/high-density lipoprotein cholesterol ratio, *NLR* neutrophils/lymphocytes ratio, *SIRI* systemic immune-inflammation index, *LACI* left atrial-ventricular coupling index

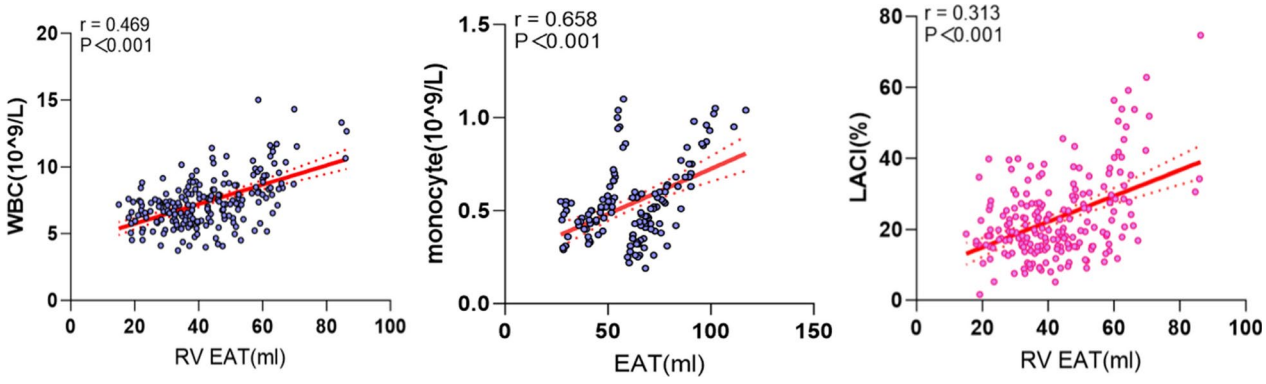

Fig. 5 Correlation between EAT and Inflammation indicators. *EAT* epicardial adipose tissue

Table 3 Univariable and multivariate coxregression analysis

Parameters	Univariable				Multivariable			
	HR	95% CI	*P* value	AIC	HR	95% CI	*P* value	AIC
LV EAT(mL)	1.054	1.022–1.088	0.001*	613.17	1.102	1.026–1.183	0.008*	593.75
EAT entropy	0.591	0.349–1.000	0.050*	620.43	0.338	0.181–0.630	0.001*	
Diabetes [n (%)]	0.412	0.256–0.663	0.000*	612.10	2.248	1.351–3.741	0.002*	
BMI (kg/m^2)	1.094	1.031–1.161	0.003*	616.31	1.086	1.018–1.159	0.012*	
Eosinophils (10*9/L)	5.087	1.676–15.438	0.004*	616.83	1.839	1.181–2.863	0.038*	
Total EAT (mL)	1.013	1.001–1.024	0.027*	624.42	0.976	0.946–1.008	0.143	
Renal failure [n (%)]	2.424	1.110–5.335	0.026*	620.49	1.118	0.427–2.930	0.820	
MHR	2.545	1.157–3.004	0.040*	620.39	0.256	0.102–0.425	0.115	
LACI (%)	1.015	0.998–1.033	0.082		–	–	–	
NHR	2.423	0.349–16.831	0.371		–	–	–	
LAESV (mL)	1.002	0.992–1.011	0.712		–	–	–	
TG (mmol/L)	1.064	0.950–1.192	0.282		–	–	–	
White blood cell (10*9/L)	1.103	0.984–1.237	0.091		–	–	–	
Neutrophils (10*9/L)	1.111	0.990–1.247	0.075		–	–	–	

BMI body mass inde, *EAT* epicardial adipose tissue, *LV* left ventricular, *LAESV* left atrial end-systolic volume, *TG* triglyceride, *MHR* mononuclear cell/high-density lipoprotein cholesterol ratio, *LACI* left atrial-ventricular coupling index

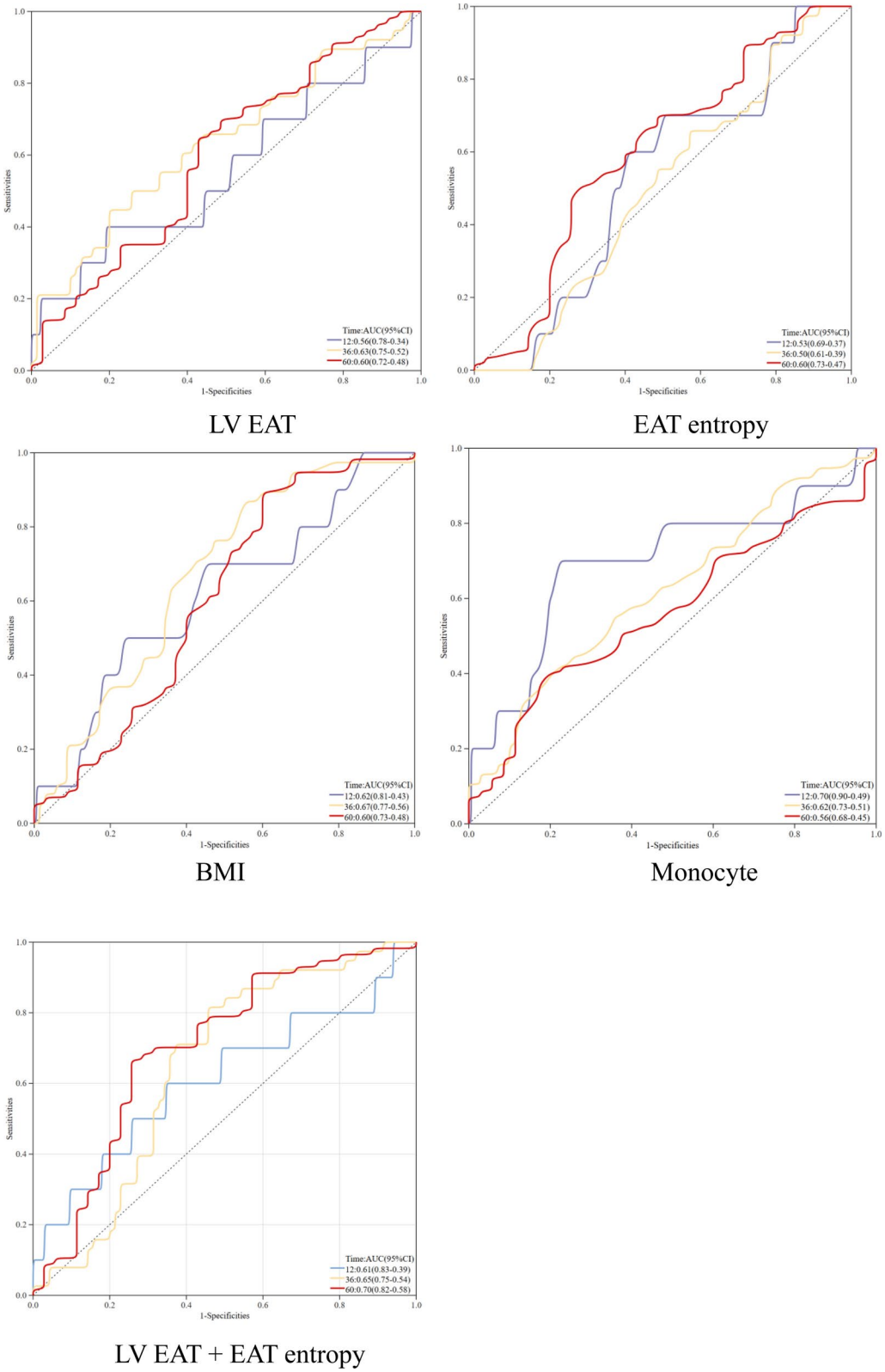

Fig. 6 ROC curve analyzing the following indicators. *EAT* epicardial adipose tissue, *LV* left ventricular, *BMI* body mass index, *AUC* area under the curve

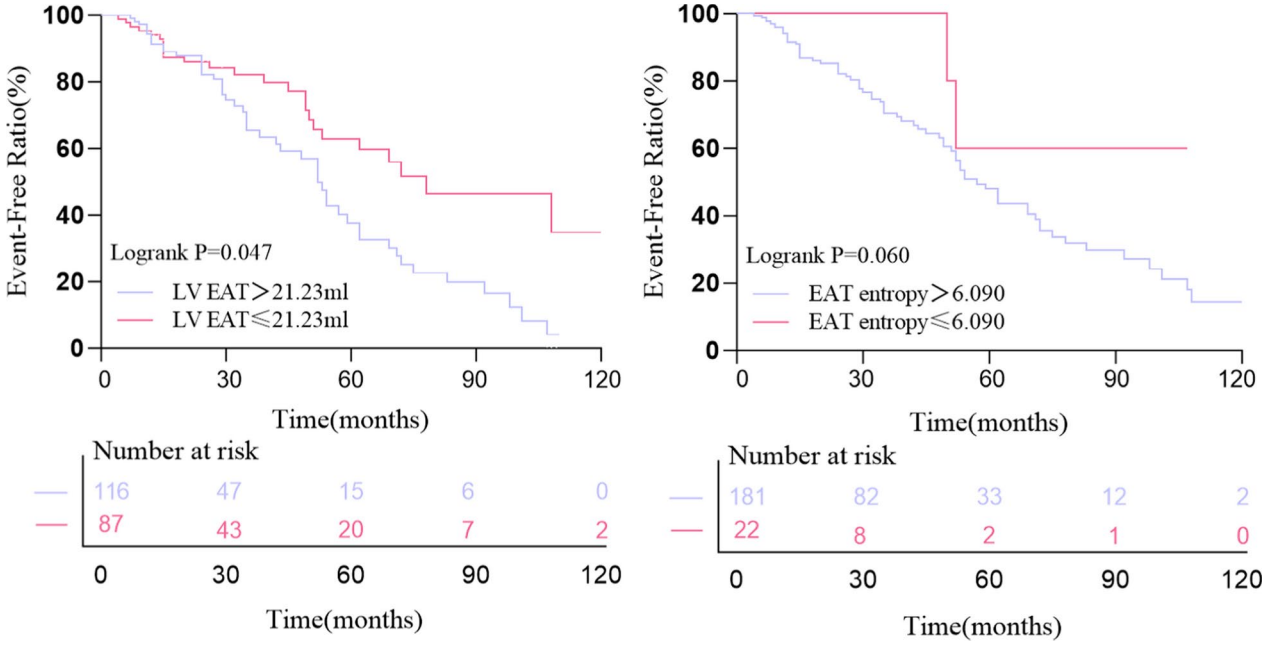

Fig. 7 Kaplan–Meier event-free survival curve of LV EAT and EAT entropy. *EAT* epicardial adipose tissue, *LV* left ventricular

obesity who develop HF typically exhibit mild increases in cardiac volume, relatively low natriuretic peptide levels, and impaired renal function, with HFpEF being the most common myocardial disease in this population [17]. HFpEF is a complex clinical syndrome that can be triggered by multiple cardiac or extracardiac conditions, such as smoking, hypertension, diabetes, renal failure, obesity, pulmonary hypertension, and coronary artery disease. It is often linked to systemic inflammation or metabolic disorders, which can directly impair coronary microvascular endothelial function [18]. The primary pathophysiological mechanisms include systemic inflammation, natriuretic peptide deficiency, neuroendocrine activation, metabolic abnormalities, and autonomic dysfunction, all of which contribute to ventricular remodeling, left ventricular diastolic dysfunction, and ventricular motion dyssynchrony [19]. BMI is a commonly used metric for assessing weight status, widely applied in epidemiological and clinical research. Although BMI has limited capacity to differentiate between muscle mass and adipose tissue, it remains an independent risk factor for various cardiovascular diseases. Research by Amir [20]indicates that both high and low BMI adversely affect prognosis in patients with MI and HF. In this study, BMI emerged as an independent predictor of HFpEF following MI, potentially due to increased BMI leading to myocardial fibrosis and electrophysiological changes that promote the development of HFpEF. There exists a close relationship between diabetes and HF, with diabetes being a significant risk factor for HF, and this risk escalates with the duration of diabetes and poor glycemic control [21]. Various mechanisms in diabetic patients can facilitate the onset of HF, including glucotoxicity, lipotoxicity, increased tissue glycation leading to myocardial fibrosis, alterations in myocardial insulin signaling associated with insulin resistance, mitochondrial dysfunction, and autonomic dysregulation. In this study, the proportion of diabetes in the HFpEF group was significantly higher than in the non-HFpEF group, with diabetes identified as an independent predictor of HFpEF following MI. This may be attributed to chronic hyperglycemia leading to the formation of advanced glycation end-products, promoting myocardial fibrosis, which in turn results in ventricular remodeling and structural microvascular changes.Furthermore, endothelial injury and reduced utilization of nitric oxide lead to endothelial dysfunction, diminished coronary blood flow reserve, and subsequently result in impaired cardiac diastolic function.

The correlation between EAT and inflammation and its role in HFpEF

A substantial body of evidence confirms that MI triggers an inflammatory response, which is primarily a coordinated physiological process [22]. Myocardial injury induces the infiltration of neutrophils and macrophages into the heart, where neutrophils and macrophages clear cellular debris and drive inflammation through the production of pro-inflammatory cytokines, further attracting additional pro-inflammatory cells. After a few days, neutrophils disappear, and macrophages emerge, while T cells regulate monocyte activation, which is crucial for cardiac healing [23]. This chronic cytokine activation and inflammatory cell infiltration can also be detected in patients with HF. EAT as a visceral fat in

direct contact with cardiomyocytes, can influence cardiac function through various mechanisms, including increased inflammation, fibrosis, autonomic nervous system dysregulation, and the mechanical effects of fibrotic fat pads. Its pro-inflammatory effects have been shown to correlate with adverse cardiovascular events. For instance, research by Mazurek [24] indicates that the accumulation of pericardial fat is associated with an increased local inflammatory state. EAT exerts direct or indirect effects on the myocardium by secreting various pro-inflammatory and anti-inflammatory mediators and cytokines, such as adiponectin, IL-6, and TNF-α. Pathological inflammatory proteins, including α1-antitrypsin and creatine kinase B-type, are also found to be elevated in HFpEF patients [25]. Baker [26] discovered increased CD45 mRNA expression in EAT from subjects with coronary artery disease, indicating enhanced macrophage infiltration, along with an increase in mast cells in the adventitia of coronary lesions, further substantiating the pro-inflammatory role of EAT. In our study, both overall and localized EAT showed a moderate positive correlation with leukocytes and monocytes, as well as a mild to moderate positive correlation between EAT volumes and the inflammatory markers MHR and SIRI.indicating the pro-inflammatory role of EAT. Moreover, inflammatory cells were significantly higher in the HFpEF group compared to the non-HFpEF group, suggesting that increased inflammatory responses in EAT can lead to direct myocardial damage, consequently elevating cardiovascular risk.Furthermore, in this study, a mild positive correlation was observed between LACI and EAT, suggesting that EAT may contribute to the progression of HFpEF by inducing diastolic dysfunction.

EAT entropy and localized EAT in relation to HFpEF

CMR allows for multi-sequence observation of cardiac alterations and provides a visual representation of adipose tissue. With advancements in faster non-breathhold sequences and highly reproducible post-processing techniques, CMR can deliver comprehensive information regarding morphology, function, perfusion, viability, and tissue characteristics in a single examination [27]. This accurate assessment of structural changes associated with HFpEF aids in identifying potential pathological causes, particularly in patients with obesity or hereditary conditions where anatomical evaluation is challenging [28]. CMR not only detects the presence and severity of MI but also offers a range of novel approaches to differentiate between infarcted, visibly damaged, and non-infarcted myocardium.

The pro-inflammatory and pro-fibrotic effects of EAT have been previously established. Wang et al. [29] demonstrated that pro-inflammatory factors secreted by EAT may promote myocardial interstitial fibrosis and ion channel dysfunction, leading to an arrhythmogenic substrate. Furthermore, EAT is rich in autonomic nerve fibers and may trigger ventricular premature beats through sympathetic overactivation. Consequently, EAT volume has a significant impact on cardiovascular diseases. However, some basic research has confirmed that the tissue structure within EAT warrants greater attention than EAT volume itself. EAT is fundamentally composed of white adipose tissue but also exhibits characteristics of brown adipose tissue. Due to the absence of fascia between EAT and myocardium, these two types of fat share the same microcirculation. In various cardiovascular diseases, the disproportionate increase of different adipose components plays distinct roles. In patients with HFpEF, white adipose tissue is dominant and more concentrated, which can directly infiltrate the myocardium through paracrine pro-inflammatory factors, leading to myocardial fibrosis and diastolic dysfunction, thereby exerting an inhibitory effect on the heart. Its increase is associated with a higher risk of cardiovascular disease [30]. In contrast, the proportion of WAT in EAT is lower in patients with HFrEF than in those with HFpEF, and its distribution is more localized. Brown adipose tissue has high metabolic efficiency, which protects the heart and helps improve cardiac function and contractility [31]. The function and morphology of EAT evolve with aging and pathological conditions, with the transition from brown to white adipose tissue being a characteristic of adult EAT. In chronic and long-term ischemic conditions, such as advanced coronary atherosclerotic heart disease, the activity of brown adipose tissue in EAT is suppressed [32]. This is evidenced by the downregulation of gene expression related to adipocyte browning and thermogenic activation, alongside an increase in the expression of pro-inflammatory cytokines. These alterations in gene expression may result in fibrosis and apoptosis of EAT in end-stage organ diseases [33]. Furthermore, the heterogeneity of EAT is evident in its structural, functional, and molecular characteristics, which exhibit spatial variations. These include differences in adipocyte size, lipid droplet morphology, and mitochondrial density. Moreover, the degree of localized macrophage and lymphocyte aggregation varies, leading to differing levels of inflammatory infiltration. Uneven collagen deposition and adipocyte necrosis within EAT contribute to varying degrees of fibrosis [34]. These findings collectively indicate the presence of tissue heterogeneity within EAT. Computed tomography (CT) can quantify the standard deviation of EAT density, reflecting the lipid/fibrosis ratio. Research suggests that this metric may, to some extent, represent the degree of inflammatory cells and fibrosis within EAT. Langenbach et al. [35]found that increased EAT density is associated with an elevated risk of cardiovascular mortality. However, the inherent spatial

resolution limitations of CT may introduce errors in density measurements.Collectively, these findings indicate the presence of tissue heterogeneity within EAT. Entropy, a novel CMR-derived parameter, can directly assess tissue homogeneity and distribution uncertainty by utilizing the entire signal intensity distribution, potentially capturing subtle changes in tissue composition within specific regions. This approach reveals numerous characteristics of the tissue at a microscopic level [36]. In our study, we employed entropy for the first time to indirectly reflect the tissue heterogeneity of EAT. Notably, we observed a reduction in EAT entropy values among patients in the HFpEF group, suggesting a decrease in the heterogeneity of EAT tissue composition. This may be attributed to the increased predominance of white adipose tissue and the distribution is more concentrated, which plays a major role, while the metabolic efficiency of protective brown adipose tissue is diminished,resulting in a poor prognosis.

The distribution of EAT throughout the heart is not uniform, with the majority of fat located around the coronary arteries and the right ventricle. Research by Corradi et al. [37] indicates that in individuals who died from non-cardiovascular causes, EAT accounts for approximately 20% of the total ventricular weight. Each region's EAT exhibits distinct transcriptomic and proteomic profiles, thereby exerting varying effects on adjacent cardiac structures [36]. For instance, the EAT surrounding the left atrium and that infiltrating the coronary arteries play different roles, specifically relating to the pathophysiology of atrial fibrillation and coronary artery disease. ISaglietto et al. [38] utilized CT-derived three-dimensional fat infiltration studies, revealing a correlation between the occurrence of atrial fibrillation and a higher degree of intramyocardial fat infiltration in the left atrium. Under physiological conditions, LV EAT provides protection to the left ventricle and coronary arteries against mechanical injury. However, in pathological states, the inflammatory factors secreted by LV EAT can diffuse directly through the pericardial fluid to the right ventricle and the surrounding area of the aorta, forming a systemic inflammatory environment that leads to myocardial fibrosis and increased left ventricular stiffness. Furthermore, LV EAT can exacerbate the degree of coronary atherosclerosis by affecting coronary blood flow and myocardial metabolism. RV EAT can alleviate the pressure on surrounding tissues during right ventricular contraction and protect the structural integrity of the right ventricle under normal conditions. However, under pathological conditions, it may affect the electrical conduction of the right ventricle and alter the electrocardiographic activity of the right ventricle. Simultaneously, the release of inflammatory and fibrotic factors from RV EAT leads to inflammation and fibrosis of the right ventricular myocardium, affecting the systolic and diastolic function of the right ventricle [39]. Recent studies have performed more detailed regionalization of EAT. For example, Kuo et al. [34]divided EAT into left atrial, right atrial, and total EAT, and the results found that left atrial EAT is an independent predictor of recurrence after atrial fibrillation ablation, and the volume of left atrial EAT is positively correlated with serum CRP levels, suggesting that EAT should be precisely localized.In our study, LV EAT demonstrated greater predictive value for the development of HFpEF in patients with MI compared to overall and RV EAT. This may be attributed to the location of EAT and the absence of fascia, allowing lipids to directly infiltrate the myocardium, with excess fatty acids derived from EAT being absorbed by myocardial cells, leading to ectopic myocardial lipid accumulation [40] and a reduction in pericardial cavity volume. This physical space limitation primarily results in LV stiffness, impaired LV diastolic function, and filling, ultimately causing HFpEF. Research by Singh et al. [41] indicates that the upregulation of gene expression for proteins involved in brown adipose activation and mitochondrial signaling within EAT is significantly associated with reduced LV mass and EAT inflammation, suggesting that increased inflammatory responses in EAT may lower brown fat metabolic rates, thereby elevating cardiovascular risk, with an increased LV mass index indicating LV hypertrophy. Seki et al. [42] found that increased EAT thickness correlates with adverse LV remodeling in patients with chronic coronary syndrome. Therefore, LV EAT likely plays a significant role in left ventricular dysfunction in conditions such as coronary artery disease and HFpEF. Further research is warranted to evaluate whether EAT can perform different functional roles based on varying pathophysiological conditions. In our study, overall EAT was not an independent predictor of HFpEF in MI patients, whereas both LV EAT and EAT entropy were identified as independent predictors, with their combined predictive efficacy being greater. This suggests that clinicians should focus on patients with MI who exhibit increased LV EAT and reduced heterogeneity, and consider targeting LV EAT as a therapeutic approach to improve patient prognosis.

Limitations (1) This investigation employed the CVI42 post-processing software to manually delineate and extract EAT and cardiac function parameters, which may demonstrate variability in quantification across different post-processing platforms. (2) This study conducted as a single-center retrospective investigation with a relatively limited sample size, exclusively enrolled cases with complete medical records while excluding those with loss to follow-up or incomplete biomarker assessments. Such methodological constraints may introduce potential selection bias, underscoring the necessity for future

multicenter prospective cohort studies to validate these preliminary findings. (3) This research primarily focuses on MI patients without stent placement, and the findings may not be generalizable to other patient populations, may constrain the generalizability of the findings. (4)The study did not systematically control for variations in medication regimens (including dosage timing and treatment modifications), which might introduce confounding effects on EAT measurements. Furthermore, the cross-sectional design precludes causal inference between observed associations.

Conclusion

In patients with chronic MI, normal LVEF, and no prior PCI, the occurrence of HFpEF is not correlated with infarct volume; however, BMI, diabetes, monocyte, LV EAT, and EAT entropy are independent risk factors for HFpEF with significant predictive value, with the highest predictive efficacy observed monocyte and when combining EAT entropy and LV EAT. Additionally, both overall and local EAT volumes exhibit a moderate positive correlation with leukocytes, monocytes and inflammatory markers, and were also positively correlated with diastolic dysfunction. This suggests that, in clinical practice, beyond traditional indicators, there should be an increased focus on EAT heterogeneity and perivascular EAT in MI patients with normal LVEF who have not undergone PCI to to reduce the incidence of HFpEF.

Abbreviations

AUC	Area under the curve
BMI	Body mass index
CMR	Cardiac magnetic resonance
EAT	Epicardial adipose tissue
HF	Heart failure
HFpEF	Heart failure with preserved ejection fraction
HFrEF	Heart failure with reduced ejection fraction
LV	Left ventricular
LVEF	Left ventricular ejection fraction
LACI	Left atrioventricular coupling index
LAESV	Left atrial end-systolic volume
MI	Myocardial infarction
PCI	Percutaneous coronary intervention
RV	Right ventricular
ROC	Receiver operating characteristic

Acknowledgements

Xin-Xiang Zhao performed the research and contributed essential tools. Yu-jiao Song and Xiao-ying Zhao analyzed the data and wrote the paper. Lu-Jing Wang assisting in data collection.Ming-tian Chen and Ting Ning edited the paper.Si-wen Chen and Pei Liu assisted in submitting articles.

Author contributions

Z.X.performed the research and contributed essential tools. S.Y. and Z.X.analyzed the data and wrote the paperW.L.assisting in data collection.C.M.and N.T. edited the paper.C.S.and L.P. assisted in submitting articles.All authors have reviewed the manuscript.

Funding

This research was supported by the Yunnan Provincial Science and Technology Platform Talent Project (Academician Expert Workstation) (202305AF150033); The Beijing Medical Award Foundation (YXJL-2022-0665-0214); and Graduate Innovation Fund of Kunming Medical University (2024S104).

Data availability

The data that support the findings of this study are available from the corresponding author, upon reasonable request.

Declarations

Competing interests

All authors have no Competing interests.

Author details

[1]Department of Radiology, The Second Affiliated Hospital of Kunming Medical University, Kunming, China

Received: 13 February 2025 / Accepted: 31 March 2025
Published online: 03 May 2025

References

1. Sun H, Kong X, Wei K, et al. Risk prediction model construction for post myocardial infarction heart failure by blood immune B cells. Front Immunol. 2023. https://doi.org/10.3389/fimmu.2023.1163350.
2. Frantz S, Hundertmark MJ, Schulz-Menger J, et al. Left ventricular remodelling post-myocardial infarction: pathophysiology, imaging, and novel therapies. Eur Heart J. 2022;43(27):2549–61. https://doi.org/10.1093/eurheartj/ehac223.
3. Carberry J, Marquis-Gravel G, O'Meara E, et al. Where are we with treatment and prevention of heart failure in patients post-myocardial infarction? JACC Heart Fail. 2024;12(7):1157–65. https://doi.org/10.1016/j.jchf.2024.04.025.
4. Mahabadi AA, Anapliotis V, Dykun I, et al. Epicardial fat and incident heart failure with preserved ejection fraction in patients with coronary artery disease. Int J Cardiol. 2022;357:140–5. https://doi.org/10.1016/j.ijcard.2022.04.009.
5. Nair N. Epidemiology and pathogenesis of heart failure with preserved ejection fraction. Rev Cardiovasc Med. 2020;21(4):531–40. https://doi.org/10.31083/j.rcm.2020.04.154.
6. Lewis GA, Schelbert EB, Miller CA. Angiotensin–neprilysin inhibition in heart failure with preserved ejection fraction. N Engl J Med. 2020;382(12):1182. https://doi.org/10.1056/NEJMc2000284.
7. Sundström J, Bruze G, Ottosson J, et al. Weight loss and heart failure: a nationwide study of gastric bypass surgery versus intensive lifestyle treatment. Circulation. 2017;135(17):1577–85. https://doi.org/10.1161/CIRCULATIONAHA.116.025629.
8. Konwerski M, Gąsecka A, Opolski G, et al. Role of epicardial adipose tissue in cardiovascular diseases: a review. Biology (Basel). 2022. https://doi.org/10.3390/biology11030355.
9. Cho DH, Park SM. Epicardial adipose tissue and heart failure, friend or foe? Diabetes Metab J. 2024;48(3):373–84. https://doi.org/10.4093/dmj.2023.0190.
10. Zhang L, Zalewski A, Liu Y, et al. Diabetes-induced oxidative stress and low-grade inflammation in porcine coronary arteries. Circulation. 2003;108(4):472–8. https://doi.org/10.1161/01.CIR.0000080378.96063.23.
11. Ren Y, Chen L, Liu J, et al. Correlation of epicardial adipose tissue and inflammatory indices in patients with STEMI and implications for atrial arrhythmias. Int J Cardiol. 2024;406:132016. https://doi.org/10.1016/j.ijcard.2024.132016.
12. Pieske B, Tschöpe C, de Boer RA, et al. How to diagnose heart failure with preserved ejection fraction: the HFA-PEFF diagnostic algorithm: a consensus recommendation from the Heart Failure Association (HFA) of the European Society of Cardiology (ESC). Eur Heart J. 2019;40(40):3297–317. https://doi.org/10.1002/ejhf.1741.
13. McDonagh TA, Metra M, Adamo M, et al. 2021 ESC Guidelines for the diagnosis and treatment of acute and chronic heart failure. Eur Heart J. 2021;42(36):3599–726. https://doi.org/10.36290/aim.2022.010.
14. Thygesen K, Alpert JS, Jaffe AS, et al. Fourth universal definition of myocardial infarction (2018). Circulation. 2018;138(20):e618–51. https://doi.org/10.1161/CIR.0000000000000617.
15. Shannon C. A mathematical theory of communication. AT&T Tech J. 2013;27(4):623–56. https://doi.org/10.1002/j.1538-7305.1948.tb00917.x.
16. Zhao X, Zhao X, Jin F, et al. Prognostic value of cardiac-mri scar heterogeneity combined with left ventricular strain in patients with myocardial infarction. J Magn Reson Imaging. 2022;58(2):466–76. https://doi.org/10.1002/jmri.28478.

17. Obokata M, Reddy YNV, Pislaru SV, et al. Evidence supporting the existence of a distinct obese phenotype of heart failure with preserved ejection fraction. Circulation. 2017;136(1):6–19. https://doi.org/10.1161/CIRCULATIONAHA.116.026807.
18. Krishnan A, Sharma H, Yuan D, et al. The role of epicardial adipose tissue in the development of atrial fibrillation, coronary artery disease and chronic heart failure in the context of obesity and type 2 diabetes mellitus: a narrative review. J Cardiovasc Dev Dis. 2022. https://doi.org/10.3390/jcdd9070217.
19. Zhang Y, Wang X, Wang P. Epicardial adipose tissue in heart failure. Adv Cardiovasc Dis. 2023;11:1010–4.
20. Amir O, Elbaz-Greener G, Carasso S, et al. Association between body mass index and clinical outcomes in patients with acute myocardial infarction and reduced systolic function: analysis of PARADISE-MI trial data. Eur J Heart Fail. 2024. https://doi.org/10.1002/ejhf.3542.
21. Echouffo-Tcheugui JB, Ndumele CE, Zhang S, et al. Diabetes and progression of heart failure: the atherosclerosis risk in communities (ARIC) study. J Am Coll Cardiol. 2022;79(23):2285–93. https://doi.org/10.1016/j.jacc.2022.03.378.
22. Swirski FK, Nahrendorf M. Cardioimmunology: the immune system in cardiac homeostasis and disease. Nat Rev Immunol. 2018;18(12):733–44.
23. Fraccarollo D, Neuser J, Moller J, et al. Expansion of CD10(neg)neutrophils and CD14(+)HLA-DR(neg/low)monocytes driving proin flammatory responses in patients with acute myocardial infarction. Elife. 2021;10:e66808.
24. Mazurek T, Zhang L, Zalewski A, et al. Human epicardial adipose tissue is a source of inflammatory mediators. Circulation. 2003;108(20):2460–6. https://doi.org/10.1161/01.CIR.0000099542.57313.C5.
25. Zhao L, Guo Z, Wang P, et al. Proteomics of epicardial adipose tissue in patients with heart failure. J Cell Mol Med. 2019;24(1):511–20. https://doi.org/10.1111/jcmm.14758.
26. Baker AR, Silva NF, Quinn DW, et al. Human epicardial adipose tissue expresses a pathogenic profile of adipocytokines in patients with cardiovascular disease. Cardiovasc Diabetol. 2006. https://doi.org/10.1186/1475-2840-5-1.
27. Meduri A, Perazzolo A, Marano R, et al. Cardiac MRI in heart failure with preserved ejection fraction. Radiol Med. 2024;129(10):1468–84. https://doi.org/10.1007/s11547-024-01874-z.
28. Friedrich MG. The future of cardiovascular magnetic resonance imaging. Eur Heart J. 2017;38(22):1698–701. https://doi.org/10.1093/eurheartj/ehx243.
29. Wang Z, Li J, Chen J, et al. Relationship between epicardial adipose tissue volume and recurrence after ablation in premature ventricular complexes. Circ J. 2023;88(7):1047–54. https://doi.org/10.1253/circj.CJ-23-0474.
30. Packer M, Lam CSP, Lund LH, et al. Characterization of the inflammatory-metabolic phenotype of heart failure with a preserved ejection fraction: a hypothesis to explain influence of sex on the evolution and potential treatment of the disease. Eur J Heart Fail. 2020;22(9):1551–67. https://doi.org/10.1002/ejhf.1902.
31. van Woerden G, Gorter TM, Westenbrink BD, et al. Epicardial fat in heart failure patients with mid-range and preserved ejection fraction. Eur J Heart Fail. 2018;20:1559–66. https://doi.org/10.1002/ejhf.1283.
32. Sacks HS, Fain JN, Cheema P, et al. Depot-specific overexpression of proinflammatory, redox, endothelial cell, and angiogenic genes in epicardial fat adjacent to severe stable coronary atherosclerosis. Metab Syndr Relat D. 2011;9(6):433–9. https://doi.org/10.1089/met.2011.0024.
33. Iacobellis G. Epicardial adipose tissue in contemporary cardiology. Nat Rev Cardiol. 2022;19(9):593–606. https://doi.org/10.1038/s41569-022-00679-9.
34. Kuo L, Wang GJ, Chang SL, et al. Feasibility of auto-quantified epicardial adipose tissue in predicting atrial fibrillation recurrence after catheter ablation. CIRC J. 2023;88(7):1089–98. https://doi.org/10.1253/circj.CJ-23-0808.
35. Langenbach IL, Hadzic I, Zeleznik R, et al. Association of epicardial adipose tissue changes on serial chest CT scans with mortality: insights from the national lung screening trial. Radiology. 2025;314(2):e240473. https://doi.org/10.1148/radiol.240473.
36. Wang L, Peng L, Zhao X, et al. Prognostic value of entropy derived from late gadolinium enhancement images to adverse cardiac events in post-myocardial infarction patients. Acad Radiol. 2022;30(2):239–47. https://doi.org/10.1016/j.acra.2022.03.021.
37. Corradi D, Maestri R, Callegari S, et al. The ventricular epicardial fat is related to the myocardial mass in normal, ischemic and hypertrophic hearts. Cardiovasc Pathol. 2004;13(6):313–6. https://doi.org/10.1016/j.carpath.2004.08.005.
38. ISaglietto A, Falasconi G, Soto-Iglesias D, et al. Assessing left atrial intramyocardial fat infiltration from computerized tomography angiography in patients with atrial fibrillation. Europace. 2023. https://doi.org/10.1093/europace/euad351.
39. 张宇,林祥玲,聂佩.心外膜脂肪组织的影像学研究进展. CT理论与应用研究. 2025;34(1):1–7. https://doi.org/10.15953/j.ctta.2024.196.
40. Wu CK, Tsai HY, Su MM, et al. Evolutional change in epicardial fat and its correlation with myocardial diffuse fibrosis in heart failure patients. J Clin Lipidol. 2017;11(6):1421–31. https://doi.org/10.1016/j.jacl.2017.08.018.
41. Singh SP, McClung JA, Thompson E, et al. Cardioprotective heme oxygenase-1-PGC1α signaling in epicardial fat attenuates cardiovascular risk in humans as in obese mice. Obesity. 2019;27(10):1634–43. https://doi.org/10.1002/oby.22608.
42. Seki H, Nakanishi K, Daimon M, et al. Epicardial fat accumulation and left heart remodelling in patients with chronic coronary syndrome. Eur Heart J Open. 2022;3(1):oeac082. https://doi.org/10.1093/ehjopen/oeac08.

Publisher's Note